Jingwei Li, Xiaolong Bai, Yanlei Li, Boyuan Ban and Jian Chen*

Effect of Ga Addition on Morphology and Recovery of Primary Si During Al–Si Alloy Solidification Refining

Abstract: The effect of Ga addition on alloy macrostructure, morphology and recovery rate of primary Si during the Al–Si–Ga alloy solvent refining process of silicon was studied in this work. The addition of Ga to Al–Si alloy could change the morphology of the primary Si. The average plate thickness of the primary Si increases with increase of Ga content. With the increase of Ga content, the average plate length of the primary Si crystals becomes larger when the Ga content is less than 5% in the Al–30% Si–*x*Ga alloy, but becomes smaller when the Ga content exceeds 5%. Al–Si–Ga alloys consist of three types, primary Si, Ga_xAl_{1-x}, (α-Al + Si + β-Ga) eutectic. (111) is the preferred growth surface of the plate-like primary Si. The recovery rate of the primary Si increases with the increase of Ga content. When the Ga content increased to 20% in Al–30%Si–*x*Ga alloy, the relative recovery rate of the primary Si increased to 50.41% than that in Al–30%Si alloy.

Keywords: Al–Si–Ga alloy, gallium addition, size distribution, primary Si, recovery rate

PACS. 81

DOI 10.1515/htmp-2014-0130
Received July 24, 2014; accepted December 4, 2014

Introduction

Photovoltaics (PV) based on solar cells, one of the cleanest methods of producing electricity, has been widely used in recent years in response to the growing demand for clean energy. Refining of metallurgical-grade silicon (MG-Si) for using as raw materials for solar cells attracts research interest due to its low material and energy cost, and more environmentally friendly technology in comparison with the traditional Siemens process [1]. The solvent refining is a purification process that relies on preferential segregation of impurities to a liquid, from which high-purity solid silicon crystals are grown [2].

Solidification refining of Si using an Al–Si solvent at low temperature has been extensively investigated [3–6]. Al–Si alloy is a typical binary eutectic system. Alloying MG-Si with Al is a process of redistribution of the impurities in silicon by taking advantage of the thermodynamic instability of the impurity elements in solid silicon at lower temperature, and the segregation ratios of the impurity elements between solid Si and Al–Si melt are less than that of it between solid Si and liquid Si. Some other metals–solvents, such as Sn [7], Ti [8] and Cu [9], have been introduced into the Al–Si solvent refining process to improve the recovery rate of the primary Si and modify the microstructure of Al–Si alloy. Maronchuk. I. E et al. [10] reported that Ga–Si solvent refining could reduce the impurity elements, such as B and P. In order to obtain the primary Si crystals, the proportion of Al–Si should be selected in the hypereutectic region. The primary Si crystal would initially precipitate from liquid alloy when the temperature of Al–Si melt decreases.However, a large content, ~12.6 wt.%, of Si is wasted during Al–Si melt cooling because of Al–Si eutectic formation. The recovery of the primary Si is limited, which remarkably reduces the economic feasibility of this process. Little work has been focused on the effect of Ga addition on the Al–Si solvent refining. From the respective fundamental research, it is necessary to investigate the effect of Ga addition on morphology and recovery of the primary Si during Al–Si alloy solidification refining and improve the refining efficiency.

The increase in the primary Si recovery rate with Ga addition was predicated considering the low content of Si in Ga–Si eutectic in the phase diagram [11] (Figure 1). In this study, Ga addition to the Al–Si melt during solidification refining was investigated to improve the recovery rate of the primary Si. The effect of Ga content variation on the alloy macrostructure and the primary Si size distribution was investigated.

***Corresponding author: Jian Chen,** Key Laboratory of Novel Thin Film Solar Cells, Institute of Plasma Physics, Chinese Academy of Science, Hefei 230031, P.R. China, E-mail: jchen@ipp.ac.cn
Jingwei Li: E-mail: ljwsilicon@163.com, **Xiaolong Bai:** E-mail: xiaolong_89@163.com, **Yanlei Li:** E-mail: ldymyy@126.com, **Boyuan Ban:** E-mail: mailboxbby@163.com, Key Laboratory of Novel Thin Film Solar Cells, Institute of Plasma Physics, Chinese Academy of Science, Hefei 230031, P.R. China

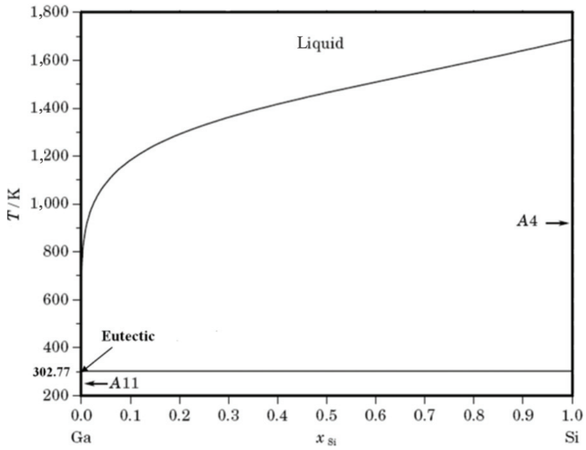

Figure 1: Ga–Si binary phase diagram.

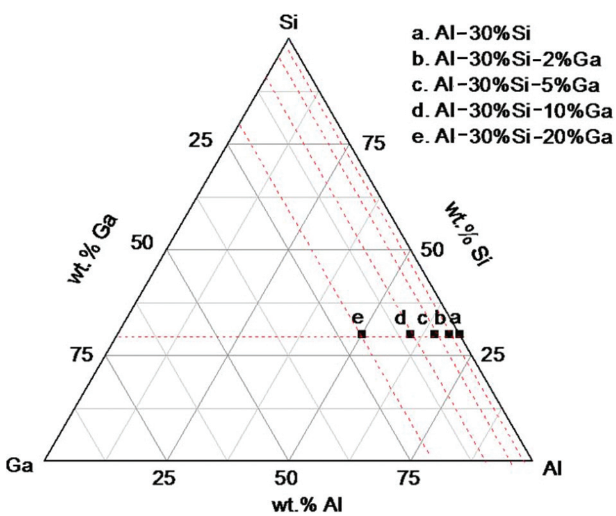

Figure 2: Compositions of Al–Si–Ga alloys in this work.

Experimental

The raw materials used to prepare the alloys were MG-Si, Al block and Ga block, and the alloy compositions are shown in Figure 2, and marked in the Al–Si–Ga ternary-phase diagram. Mass fractions of impurities in MG-Si, Ga and Al are shown in Table 1. The content of Si in Al–Si–Ga alloy was fixed at 30%, but the content of Ga varies (2%, 5%, 10% and 20%). Figure 3 shows the flow-chart of solvent refining process of MG-Si. The MG-Si, Al and Ga block samples were placed in an SiC electric resistance furnace, which was connected to a proportional–integral–derivative (PID) controller with a Pt/Pt–10%Rh thermocouple, maintaining thermally equilibrium at 1,473 K, which was above the corresponding liquidus temperature of the alloys, held for 7.2×10^3s in Ar atmosphere and then cooled down to room temperature at a rate of 8.3×10^{-3} K/s. Then, all samples were cut into two halves and one-half of each sample was polished for macro- and micro-structure analysis. The left half was treated with hydrochloric acid leaching to obtain the Si particles (primary Si and eutectic Si). A 5 g sample of Al–Si–Ga alloy was immersed in hydrochloric acid (12 mol/L) at 353 K for 8.64×10^4 s. After acid leaching, the solution was filtered and the silicon particles were rinsed thoroughly with deionized water and then dried. The Si particles were screened with a 35 mesh sieve to obtain the primary Si grains. The primary Si grains

Table 1: Mass fraction of impurities in MG-Si, Ga and Al (ppmw).

	B	P	Al	Fe
MG-Si	25	43	2,434	2,818
Ga	0.93	3.13	5.72	8.77
Al	7	35	Main	9,279

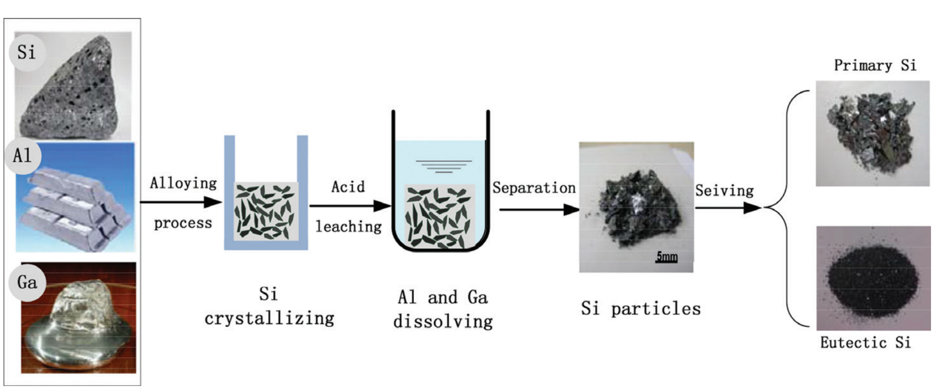

Figure 3: Flowchart of solvent refining process of MG-Si.

were analyzed by optical microscope (OM), scanning electron microscope (SEM) and X-ray diffraction (XRD).

Results and discussion

Figure 4 shows the cross-sectional microstructure of the Al–Si and the Al–Si–Ga alloys solidified at a cooling rate of 8.3×10^{-3} K/s. As can be seen from that, for Al–30%Si alloy, the needle-like primary Si grains were uniformly distributed and surrounded by eutectics in the entire alloy shown in Figure 4(a). No Si floatation was observed. For the Al–Si alloy, the variation of Si content generated the distribution change of the primary Si. Jiayan Li et al. [12] reported that the primary Si crystals are distributed at the bottom and the edge of the Al–22.8%Si alloy sample, while in the middle, no primary Si crystals are found. In our previous work [13], the primary Si crystals distribute more uniformly in the Al–35%Si alloy without super gravity. Therefore, it can be concluded that the distribution of the primary Si crystals becomes more uniform for hypereutectic alloys with the increase of Si content in the Al–Si alloys. When Ga was added into the Al–Si alloys, the distribution of the primary Si is also uniform in the entire alloy as shown in Figure 4b–d. Although the density of solid Si (2.3×10^3 kg/m^3) is less than that of the Si–Al melt ($\sim 2.4 \times 10^3$ kg/m^3) [14] or Ga melt($\sim 5.1 \times 10^3$ kg/m^3), the high viscosity of the melt makes the primary Si crystals dispersed uniformly in the Al–Si–Ga alloy.

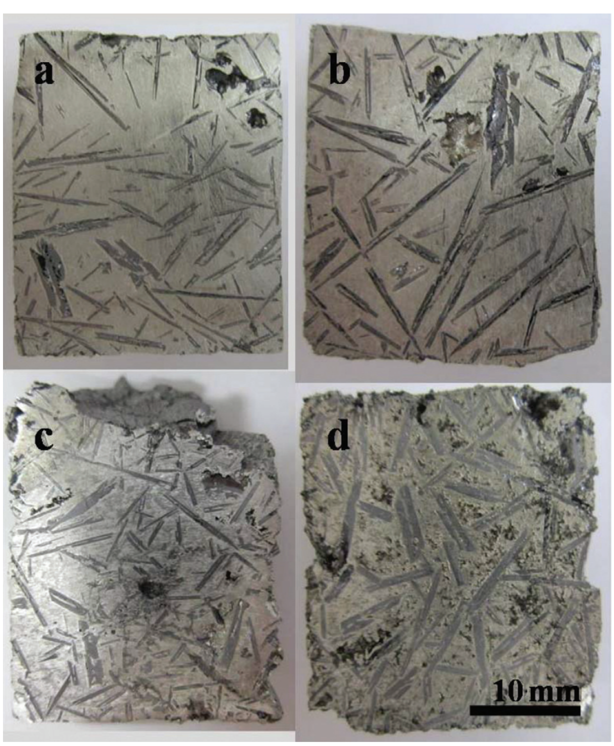

Figure 4: Macrostructures of Al–Si alloy with different Ga contents: (a) Al–30%Si,(b) Al–30%Si–5%Ga, (c) Al–30%Si–10%Ga, (d) Al–30%Si–20%Ga.

Figure 5 shows the images of plate-like primary Si particles. As can be seen from that, the sizes and shapes of plate-like primary Si particles are not constant. The number of plate-like primary Si particles is too large, and it is difficult to accurately define the primary Si from the three-dimensional angle. In order to describe the size of the plate-like primary Si, the thickness and the length of the primary Si in the cross section of the alloy are statistically counted by image analysis.

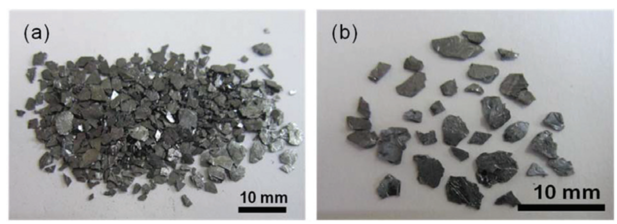

Figure 5: Images of plate-like primary Si particles of Al–30%Si–20%Ga alloy.

With the addition of Ga, the variations of the thickness and the length of Si plate is confirmed by the image analysis, which is shown in Figure 6a and b. In Figure 6a, with the increase of Ga content in the Al–Si–Ga alloys, the plate thickness of the primary Si crystals increases. When the Ga content is 0, i.e. Al–30%Si alloy, the plate thickness of the primary Si crystals is 0.50 ± 0.21 mm. When the Ga content is 2% in the Al–30%Si–xGa alloy, the primary Si thickness is also 0.50 ± 0.21 mm, which is equal to the thickness of that in Al–30%Si alloy. However, the primary Si length (6.73 ± 2.53 mm) in Al–30%Si–2%Ga alloy is larger than that (6.19 ± 2.48 mm) in Al–30%Si alloy. As for Al–30%Si–20%Ga alloy, the thickness of that is 0.70 ± 0.25 mm. However, the variation of the length of the primary Si crystals is not consistent with the trend of the thickness. With the increase of Ga content, the average length of the primary Si crystals becomes larger when the Ga content is less than 5% in the Al–30%Si–xGa alloys, but when the Ga content exceeds 5%, the average length of the primary Si crystals decreases, which is shown in Figure 6b. For Al–30%Si alloy, the length of the primary Si is 6.19 ± 2.48 mm. When the Ga content is 5%, the length of the primary Si crystals is 8.49 ± 3.72 mm, but the length of that is 4.83 ± 1.52 mm for Al–30%Si–20%Ga alloy. Jiayan Li et al. [7, 15] have investigated effect of Sn addition on the primary Si recovery in Si–Al melt during solidification refining of silicon, and experimental results also

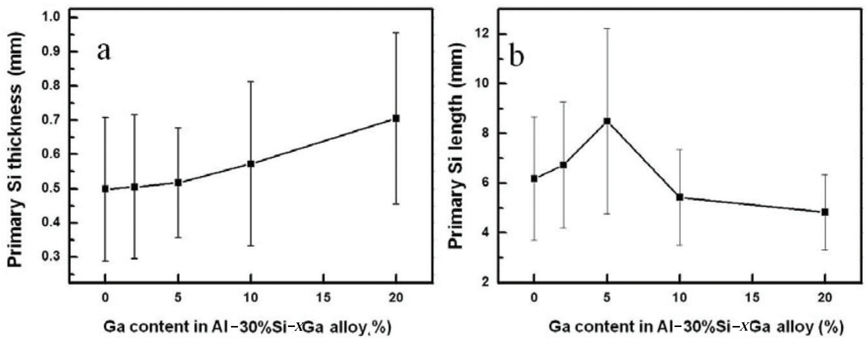

Figure 6: Plate thickness and length of primary Si as a function of Ga content (a) thickness, (b) length.

demonstrated that with the addition of metal Sn, the thickness of the Si plates increases. Therefore, the addition of metal on Al–Si alloy could increase the thickness of the Si plates to some extent.

As for the reason of thickness variation, it can be explained as follows. First, the refining temperature of the alloy decreased with the addition of Ga. For Al–30% Si alloy, the liquidus temperature of Al–30%Si alloy is 1,010 K [16], and the melting point of Ga is 303 K [11]. After the introduction of Ga, the liquidus temperature of Al–30%Si–xGa alloy was lower than that of Al–30%Si alloy. The precipitation duration of the primary Si was prolonged, which maintained the precipitation process and made sufficient growth of the plate-like primary Si along specific crystallographic orientation to obtain longer primary Si. Second, viscosity is of particular importance for considering the relationship between convection and solidification of melt. The melt convention increases and the viscosity of alloy decreases with the addition of Ga. In literature, the viscosity of Ga is 0.436 mPas [17]. However, for Al–Si hypereutectic alloy, viscosity increases with decrease in temperature. For example, in Al–16%Si alloy, the viscosity of the melt was in the range of 0.5–0.65 mPas when the temperature was between 1,223 and 973 K [18]. After the addition of Ga, the viscosity of the melt could be decreased to some extent, which increases the convection of the Al–Si–Ga melt and promotes the precipitation of the primary Si to obtain the large size plate-like primary Si.

Figure 7 shows the SEM micrograph of Al–30%Si–5% Ga alloy, and EDS line analysis demonstrates that it is divided into three main phases. The microstructure

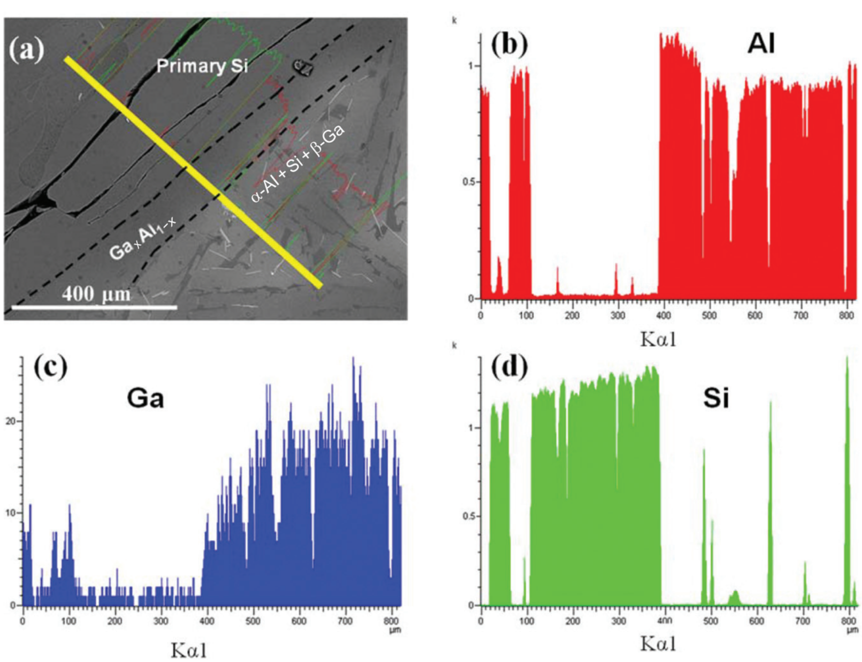

Figure 7: SEM micrograph of Al–30%Si–5%Ga and EDS line profiles of Al, Ga and Si, respectively.

contains primary Si, Ga_xAl_{1-x}, (α-Al + Si + β-Ga) eutectic. The phases with gray color are primary Si, the dark gray phases at the boundary of the primary Si are Ga_xAl_{1-x} phase, and the light color phases are mixture of Si, α-Al and β-Ga, which could be identified by EDS shown in Figure 4b–d. During the solidification process of the Al–Si–Ga ternary alloy, the primary Si grows from the melt first, because of the high melting point of Si and low solubility of Si in Al and Ga. And then the binary Ga_xAl_{1-x} forms, followed by the solidification of the ternary eutectic α-Al + Si + β-Ga. Compared with the binary Al–Si alloy, the primary Si in the Al–Si–Ga alloys becomes shorter and thicker with the increase of Ga content.

The relationship between Ga content in the Al–Si–Ga alloy and the recovery rate of Si is plotted in Figure 8. The alloy samples were dissolved by HCl solution to obtain the purified Si, which contains the plate-like primary Si grains and powdery eutectic Si. The Si particles were screened with a 35 mesh sieve to obtain the primary Si. The total recovery rate of Si refers to the ratio between the Si mass (primary Si and eutectic Si) and the alloy mass. As can be seen from Figure 8, the total recovery rate of Si was kept in the range of 25–30% with the increase of Ga content. The experimental result was close to the theoretical total recovery rate of 30%, which was abided by the law of mass conservation. However, as compared with Al–30%Si, the recovery rate of the primary Si was decreased first and then increased with the increase of Ga content in the Al–30%Si–xGa alloy.When the Ga content was less than 10% in the Al–30%Si–xGa alloy, the recovery rate of the primary Si was less than that in the Al–30%Si alloy. Then, when the Ga content was higher than 10% in the Al–30% Si–x%Ga alloy, the recovery rate of the primary Si was larger than that in the Al–30%Si alloy. For Al–30%Si alloy, the recovery rate of primary Si was 16.90%. When the Ga content increased to 20% in Al–30%Si–xGa alloy, the recovery rate of the primary Si was 25.42%. The relative recovery rate of the primary Si increased to 50.41% than that in Al–30%Si alloy. These results indicated that Ga could refine the primary Si grains. With the increase of Ga content, the average size of the primary Si grains also became larger, which increased the recovery rate of the primary Si. At the same time, according to the mass conservation, the recovery rate of the eutectic Si was the subtraction between the total recovery rate of Si and that of the primary Si. Therefore, the opposite variation trend on the recovery rate of the eutectic Si was shown in Figure 8. As can be seen from that, the increase in the recovery rate of the primary Si is significant with the increase of Ga. This result indicates that it is beneficial to improve the recovery rate of the primary Si with Ga addition.

After acid leaching and sieving, the solvent of Ga, Al and partial Si are dissolved, leaving the plate-like primary Si crystals. XRD analysis demonstrates that the plate-like primary Si is crystalline Si with <111> crystallographic orientation shown in Figure 9, which indicated that (111) is the preferred growth surface. X. Gu et al.[3] also reported the <111> crystallographic orientation of the purified Si from Al-Si melt. This is in agreement with the current experiment results. It also shows that the addition of Ga in the Al–Si alloys does not change the preferred growth surface of the primary Si plates. As for the removal effect of impurities, much more work need to be done in future.

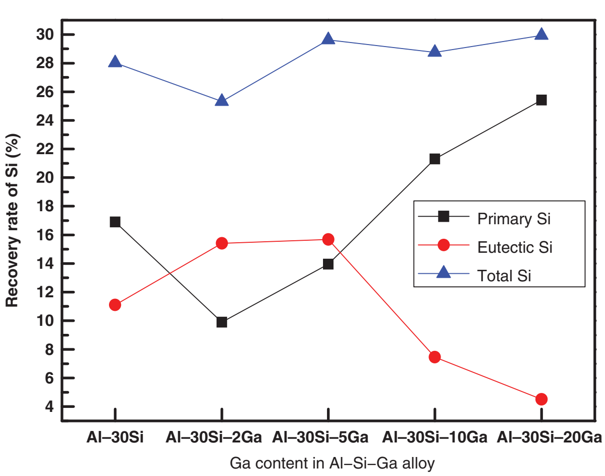

Figure 8: Relationship between Ga content in Al–Si–Ga alloy and recovery rate of Si.

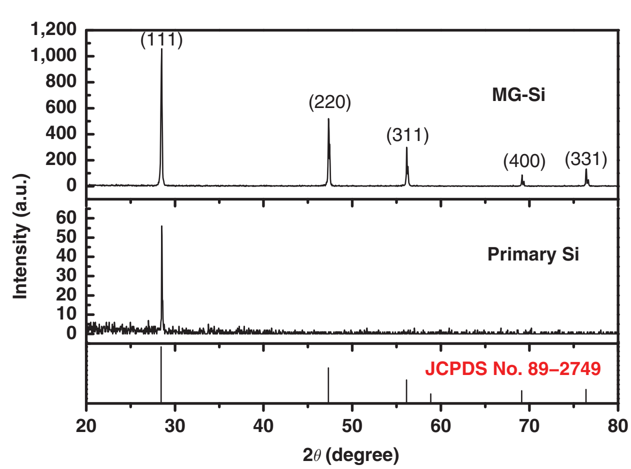

Figure 9: XRD patterns of MG-Si and primary Si after Al–30% Si–5% Ga alloy solvent refining.

Conclusions

The addition of Ga to the Al–Si alloy could change the morphology of the primary Si phase. The plate thickness of the primary Si plates in Al–Si–Ga alloy increases with the increase of Ga content. With the increase of Ga content, the average length of the primary Si crystals became larger when the Ga content is less than 5% in the Al–30% Si–*x*Ga alloy, but becomes smaller when the Ga content exceeds 5%. Al–Si–Ga alloy consisted of three types of microstructure and the microstructure contains primary Si, Ga_xAl_{1-x}, (α-Al + Si + β-Ga) eutectic. The (111) surface is the preferred growth surface of the plate-like primary Si. When the Ga content increased to 20% in Al–30%Si–*x*Ga alloy, the relative recovery rate of the primary Si increased to 50.41% than that in Al–30%Si alloy. The increase in the primary Si recovery rate is significant with the increase of Ga, which indicates that it is beneficial to improve the recovery rate of the primary Si.

Acknowledgments: This work was financially supported by National Natural Science Foundation of China (No. 51404231 and 51474201); Anhui Provincial Natural Science Foundation (No. 1508085QE81); China Postdoctoral Science Foundation (No. 2014M561846); 100 Talent Program of Chinese Academy of Sciences; Science Fund of Institute of Plasma Physics, Chinese Academy of Sciences, under Grant Nos 095YZ31222 and Y35QT10894.

References

1. Sergio P. Thermodynamic evaluation of segregation behaviors of metallic impurities in metallurgical grade silicon during AlSi solvent refining process. Sol Energy Mater Sol Cells 2010;94:1528–33.
2. Li JW, Guo ZC, Li JC, Yu LZ. Thermodynamic evaluation of segregation behaviors of metallic impurities in metallurgical grade silicon during AlSi solvent refining process. J Cryst Growth 2014;394:18–23.
3. Gu X, Yu X, Yang D. Low-cost solar grade silicon purification process with Al–Si system using a powder metallurgy technique. Sep Purif Technol 2011;77:33–9.
4. Yoshikawa T, Morita K. Refining of silicon during its solidification from a Si–Al melt. J Cryst Growth 2009;311: 776–9.
5. Yu WZ, Ma WH, Lü GQ, Ren YS, Xue HY, Dai YN. Si purification by enrichment of primary Si in Al–Si melt. Trans Nonferrous Met Soc 2013;23:3476–81.
6. Li JW, Guo ZC, Tang HQ, Li JC. Removal of Impurities from Metallurgical Grade Silicon by Liquation Refining Method. High Temp Mater Processes 2013;32:503–10.
7. Li J, Liu Y, Tan Y, Li Y, Zhang L, Wu S, et al. Effect of tin addition on primary silicon recovery in Si–Al melt during solidification refining of silicon. J Cryst Growth 2013;371:1–6.
8. Yoshikawa T, Morita K. Removal of B from Si by Solidification Refining with Si–Al Melts. Metall Mater Trans B 2005;36: 731–6.
9. Yoshikawa T, Morita K. Thermodynamics of solid silicon equilibrated with Si–Al–Cu liquid alloys. J Phys Chem Solids 2005;66: 261–5.
10. Maronchuk IE, Solovyev OV, Khlopyonova IA. A new method of metallurgical silicon purification. Funct Mater 2005;12:596–9.
11. Olesinski RW, Kanani N, Abbaschian GJ. The Ga-Si (Gallium-Silicon) System. Bull Alloy Phase Diagr 1985;6: 362–4.
12. Li J, Jia P, Li Y, Cao P, Liu Y, Tan Y. Effect of Zn addition on primary silicon morphology and B distribution in Si–Al alloy. J Mater Sci Mater Electron 2014;25:1751–6.
13. Li JW, Guo ZC, Tang HQ, Wang Z, Sun ST. Si purification by solidification of Al–Si melt with super gravity. Trans Nonferrous Met Soc 2012;22:958–63.
14. Yoshikawa T, Morita K. Refining of silicon by the solidification of Si–Al melt with electromagnetic force. ISIJ Int 2005;45: 967–71.
15. Li Y, Tan Y, Li J, Xu Q, Liu Y. Effect of Sn content on microstructure and boron distribution in Si–Al alloy.J Alloys Compd 2014;583:85–90.
16. Murray JL, McAlister AJ. The Al–Si (Aluminum-Silicon) System. Bull Alloy Phase Diagr 1984;5:74–84.
17. Battezzati L, Greer AL. The viscosity of liquid metals and alloys. Acta Metall 1989;37:1791–802.
18. Geng HR, Wang R, Yang ZX, Chen JH, Sun CJ, Wang Y. Temperature dependence of viscosity of Al–Si alloy melts. Acta Metall Sin 2005;18:159–63.